



Contents lists available at ScienceDirect

Dental Materials

journal homepage: www.elsevier.com/locate/dental

Fatigue behaviour of a self-healing dental composite

Ke Ning^a, Fang Yang^a, Ewald Bronkhorst^b, Jan Ruben^b, Liebert Nogueira^c, Håvard Haugen^c, Bas Loomans^b, Sander Leeuwenburgh^{a,*}^a Radboud University Medical Center, Radboud Institute for Molecular Life Sciences, Department of Dentistry, Regenerative Biomaterials, Philips van Leydenlaan 25, Nijmegen, the Netherlands^b Radboud University Medical Center, Radboud Institute for Health Sciences, Department of Dentistry, Restorative Dentistry, Philips van Leydenlaan 25, Nijmegen, the Netherlands^c University of Oslo, Institute of Clinical Dentistry, Department of Biomaterials, Oslo 0317, Norway

ARTICLE INFO

Keywords:

Self-healing composites
 Fatigue behaviour
 Staircase test
 Chewing simulator (Rub&Roll)
 Fatigue strength
 Flexural strength

ABSTRACT

Objective: Novel self-healing resin-based composites containing microcapsules have been developed to improve the mechanical performance of dental restorations. However, the long-term fatigue behaviour of these self-healing composites has still been hardly investigated. Therefore, this manuscript studied the fatigue behaviour of self-healing composites containing microcapsules by subjecting the specimens to traditional staircase tests and ageing in a custom-designed chewing simulator (Rub&Roll) to simulate oral ageing physiologically relevant conditions.

Methods: To prepare self-healing composite, poly(urea-formaldehyde) microcapsules containing acrylic self-healing liquids were synthesized. Subsequently, these microcapsules (10 wt%) and initiator (benzoyl peroxide, BPO, 2 wt%) were incorporated into a commercial flowable resin-based composite. Microcapsule-free resin-based composites with and without BPO were also prepared as control specimens. A three-point flexural test was used to measure the initial flexural strength (S_{initial}). Subsequently, half of the specimens were used for fatigue testing using a common staircase approach to measure the fatigue strengths (FS). In addition, the other specimens were aged in the Rub&Roll machine for four weeks where after the final flexural strength (S_{final}) was measured.

Results: Compared to S_{initial} , FS of all tested specimens significantly decreased as measured through staircase testing. After 4 weeks of ageing in the Rub&Roll machine, S_{final} was significantly reduced compared to S_{initial} for microcapsule-free resin-based composites, but not for the self-healing composites ($p = 0.3658$). However, the self-healing composites are still in the experimental phase characterized by a low mechanical strength, which still impedes further clinical translation.

Significance: Self-healing composites containing microcapsules exhibit improved fatigue resistance compared to microcapsule-free non-self-healing composites.

1. Introduction

Based on principles of minimally invasive dentistry, direct resin-based dental composites are routinely applied in restorative dentistry worldwide [1,2]. Nevertheless, the oral environment is complex and highly challenging, characterized by cyclic loading under wet conditions. One of the main failure reasons of resin-based restoration is fracture based on a meta-analysis study [3]. These challenging conditions induce the formation of microcracks in the resin matrix, which may

arise due to silane hydrolysis and/or plasticizing of resin components [4, 5].

Continuous mechanical and environmental stress can lead to crack propagation, resulting in catastrophic failure of resin-based dental composite restorations [5–7]. To overcome this drawback, self-healing dental composites containing microcapsules filled with polymerizable healing liquid have been designed [8–11]. The self-healing ability of such dental composites has been confirmed under static conditions both by our and other groups [8,9,11–13]. However, these static

* Correspondence to: Radboud University Medical Center, Radboud Institute for Molecular Life Sciences, Department of Dentistry, Regenerative Biomaterials, Philips van Leydenlaan 25, 6525 EX Nijmegen, the Netherlands.

E-mail address: Sander.Leeuwenburgh@radboudumc.nl (S. Leeuwenburgh).

<https://doi.org/10.1016/j.dental.2023.08.172>

Received 6 September 2022; Received in revised form 10 August 2023; Accepted 16 August 2023

0109-5641/© 2023 The Author(s). Published by Elsevier Inc. on behalf of The Academy of Dental Materials. This is an open access article under the CC BY license (<http://creativecommons.org/licenses/by/4.0/>).

measurements do not correspond to physiological loading scenarios [12, 14,15]. Evidently, static mechanical tests do not permit to characterize of long-term fatigue behaviour of self-healing dental composites [14, 16]. Nevertheless, this long-term fatigue behaviour of self-healing dental composites has received surprisingly little attention. To the best of our knowledge, only one study has focused on the characterization of fatigue behaviour of self-healing dental composites [17]. The fatigue behaviour of conventional non-self-healing resin-based composites, on the other hand, has been extensively studied using various cyclic loading tests [5,15,18]. Among them, staircase testing was shown to be an effective method to determine the fatigue strength of resin-based composites using the approximation described by Dixon and Mood [19]. Besides cyclic loading caused by mastication, the ageing environment also strongly determines the fatigue resistance of dental resin-based composites [5,20,21]. Wet conditions, including enzymes from the saliva, can strongly reduce the mechanical performance of resin-based composites [21,22]. We recently designed a new in vitro fatigue/wear (ageing) simulation (Rub&Roll) machine to study the influence of cyclic loading and the wet oral environment simultaneously. This machine applies cyclic grinding stresses resembling physiological loading conditions in terms of stress magnitude and frequency and allows to test cyclic loading under wet conditions closely resembling the oral environment [23,24]. Using this chewing simulation machine, experimental materials can be subjected to high numbers of chewing cycles corresponding to several years of physiological loading in just a few weeks. In addition, our previous studies showed that the cup-shape wear patterns created by Rub&Roll on molars closely resembled those on molar occlusions of human patients [25]. Based on the favorable combination of flexibility and practicality, this machine enables to study fatigue behaviour of dental restorative materials under physiologically relevant in vitro conditions [23,26].

We hypothesized that our self-healing resin-based composites containing microcapsules filled with healing liquid would exhibit enhanced fatigue resistance compared to non-self-healing controls. To test this hypothesis, the current study investigated the fatigue resistance of these self-healing resin-based dental composites using two different experimental setups: 1) traditional staircase fatigue tests; and 2) fatigue testing using a wear simulation device (Rub&Roll) to simulate oral ageing under conditions combining cyclic loading and a wet environment.

2. Materials and methods

2.1. Synthesis of microcapsules

We used an oil-in-water method to synthesize poly(urea-formaldehyde) (PUF) microcapsules containing an acrylic healing liquid as previously reported [12]. The “water phase” was an aqueous solution of ethylene-maleic anhydride (EMA, Sigma, UK), and the “oil phase” was the healing liquid composed of triethylene glycol dimethacrylate (TEGDMA, Sigma-Aldrich, Switzerland) and N, N-Dimethyl-p-toluidine (DEPT, Merck KGaA, India). Urea (Sigma, UK) and formaldehyde solution (37 wt%, Sigma, Switzerland) were used to form the microcapsule shell. First, at room temperature, 26 mL (2.5 wt%) EMA solution was added to 100 mL Milli-Q water. A lab mixer (IKA Works (Asia), RW20 DZM. N, Sdn. Bhd. Malaysia) with a three-bladed propeller (radius: 20 mm) was used to stir the solution at 300 rpm. Subsequently, 2.5 g urea, 0.25 g ammonium chloride (Merck KGaA, Germany), and 0.25 g resorcinol (Sigma-Aldrich, India) were added to this aqueous solution. Ammonium chloride and resorcinol were used to improve the strength and toughness of the microcapsules [27]. 40 mL self-healing liquid (mixture of TEGDMA 99 wt% and DEPT 1 wt%) was added dropwise to the solution using a single syringe infusion pump (KDS, Infusion), where after the stirring speed and pH were adjusted to 400 rpm and 3.5. Subsequently, 6.3 g formaldehyde solution was added to this emulsion to form the microcapsule shells. Thereafter, the emulsion was left 4 h in a water-bath at 55 °C to allow for polymerization of

Table 1
Composition of various experimental groups.

| Group name | Initiator (BPO) concentration (wt %) | Microcapsule concentration (wt %) | Flowable composite (wt %) |
|--------------------------------------|--------------------------------------|-----------------------------------|---------------------------|
| Resin-based composite | 0 | 0 | 100 |
| Resin-based composite containing BPO | 2 | 0 | 98 |
| Self-Healing composite | 2 | 10 | 88 |

the microcapsule shells, after which the emulsion was cooled down and the microcapsules were filtered using a vacuum filter. Finally, the microcapsules were washed with water and acetone and air-dried in a fume hood at room temperature for 24 h. To minimize potential damage to the microcapsules, we washed these microcapsules using water and acetone alternately for short time periods.

2.2. Characterization of microcapsules

Light microscopy (LM, Zeiss) and scanning electron microscopy (SEM, Sigma 300, Zeiss) were used to characterize the morphology of the microcapsules. The microcapsule size and shell thickness were measured based on the LM images and SEM images (Imaging software Fiji, Image J 1.47 v). Microcapsule size was measured by counting 100 microcapsules randomly from 5 pictures. To confirm successful encapsulation of the healing liquid in the microcapsules, we used Fourier-transform infrared spectroscopy (FTIR, Spectrum Two, PerkinElmer) to characterize the molecular structure of the microcapsules resolution at 4 cm⁻¹, averaging three scans.

2.3. Preparation of composite specimens

All composite specimens were prepared using rectangular molds (polydimethylsiloxane, PDMS) with 12.5 × 5 × 2.5 mm dimensions. A commercially available flowable composite (Clearfil Majesty™ ES Flow, Kuraray, Osaka, Japan), is a bisphenol A-glycidyl methacrylate based light-cured composite with silanated barium glass filler (78 wt%, 66 vol %, 0.37 –1.5 μm) [28], a white powder-phase initiator (benzoyl peroxide, BPO, ACROS, New Jersey, USA), and self-healing microcapsules were used for composite specimen preparation. Under the current experimental conditions, the addition of additional BPO did not affect the polymerization process of the composite specimens. Based on our previous study, microcapsules of ~200 μm were chosen to achieve maximum self-healing efficiency [12]. Table 1 provides the composition of the various experimental groups.

For the resin-based composites containing BPO as well as the self-healing composites, additional weighing and mixing procedures were required before transferring the composites into the molds. To ensure that the flowable composites were not prematurely exposed to light, tinfoil paper was used to cover the flowable composite to prevent light exposure as much as possible during the weighing and subsequent manual mixing. We gently manually mixed the microcapsules and initiator successively into the flowable composite to prepare composite specimens in the plastic weighing boat with a dental probe (for 20–30 s).

All the composites were transferred into the rectangular molds and covered with histology glass slides to achieve a smooth top surface on each specimen. Every specimen was cured for 20 s on the top side directly through the histology glass slide and then on the bottom side without the mold for 20 s again with a LED polymerization unit (Blue-phase 16i, Ivoclar, Schaan, Liechtenstein, output >1300 mW/cm²). All specimens were stored in distilled water for 24 h at room temperature before mechanical testing.

Table 2

The initial stress, step size and group size in staircase method.

| Group | Initial stress (MPa) | Step size (ΔS) (MPa) | Group size (N) |
|-------|----------------------|--------------------------------|----------------|
| 1 | 70 | 15 | 15 |
| 2 | 50 | 15 | 15 |
| 3 | 25 | 5 | 15 |

2.4. Flexural strength

A universal testing machine (AMETEK, LS5, LLOYD) was used to determine the flexural strength of the specimens using a three-point-bending test (span: 10 mm, crosshead speed: 1 mm / min) [8]. Initial flexural strength (S_{initial}) and final flexural strength (S_{final}) were calculated using the formula (1) ($N = 8$):

$$S = \frac{3LP_{\max}}{2bh^2} \quad (1)$$

where L is the span, P_{\max} the maximum loading force, b the width of specimen, and h the thickness of specimen.

2.5. Fatigue test by the staircase method

Fatigue resistance of the resin-based composite specimens was determined using a previously described staircase method [19,29] at room temperature using a universal testing machine (858 Mini Bionix II, MTS) according to a cyclic three-point bending test setup (span: 10 mm). The initial stress amplitude (~50% of the initial maximum flexural strength S_{initial}) [19,29], step size (in the range of 0.5 ~ 2 times of the standard deviation of S_{initial}), and group size of the staircase method are

shown in Table 2. The universal testing machine was set at a frequency of 1 Hz and the duration of the fatigue test was fixed at 10,000 cycles [15]. The first specimen was tested at the initial stress until it either failed or survived the 10,000 cycles to start the staircase fatigue test in each group. According to the principle of staircase testing, the load applied on the second specimen was decreased or increased by the predetermined step size (ΔS) depending on if the previously tested sample failed or survived the fatigue test, respectively. Finally, the staircase fatigue test was finished until all specimens were tested according to the procedure above.

After the testing, the mean fatigue strength (FS, μ , formula (2)) and standard deviation (σ , formula (3) or (4)) were calculated by the Dixon and Mood method [30]. The corresponding formulas are shown below:

$$\mu = S_0 + \Delta S \left(\frac{A}{F} \pm \frac{1}{2} \right) \quad (2)$$

$$\sigma = 1.62\Delta S(F_{BA} + 0.029) \text{ if } F_{BA} \geq 0.3, \quad (3)$$

$$\text{or } \sigma = 0.53\Delta S \text{ if } F_{BA} < 0.3 \quad (4)$$

$$F_{BA} = \frac{FB - A^2}{F^2}$$

$$A = \sum_{j=0}^{j_{\max}} j \times n_j$$

$$B = \sum_{j=0}^{j_{\max}} j^2 \times n_j$$

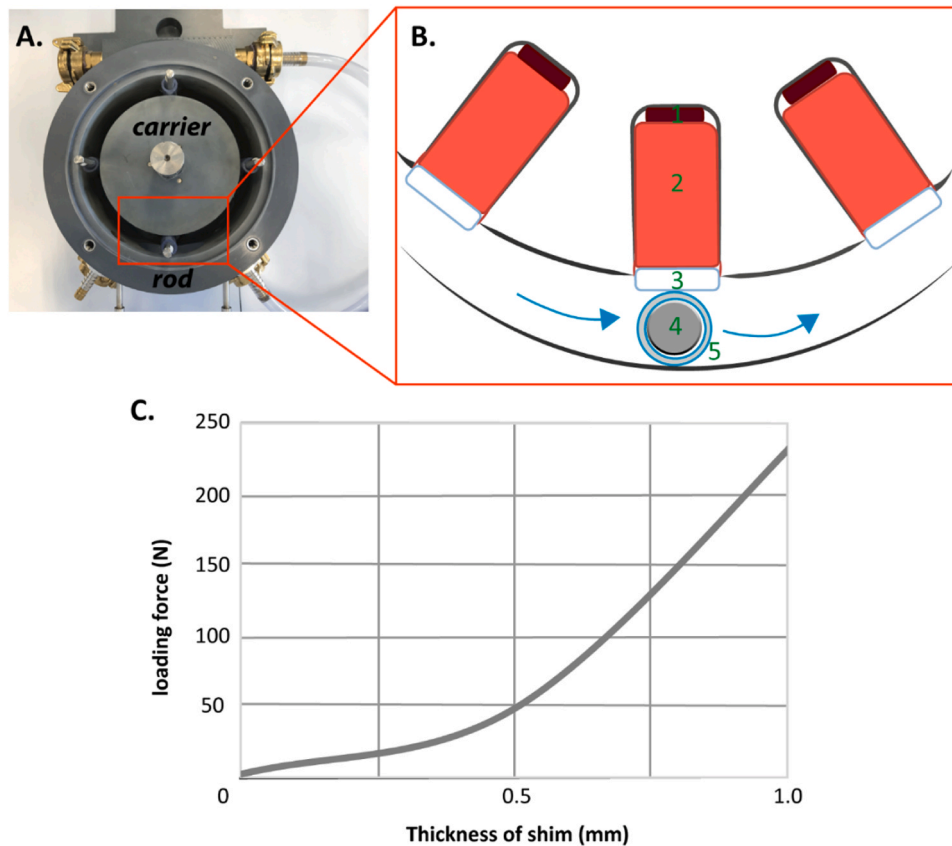


Fig. 1. Image of the interior of the wear simulating machine (Rub&Roll) including a sample carrier in the center and four rods around the carrier (A); schematic partial cross-section of sample holders in the Rub&Roll machine (B), including the shim (1), poly(methyl methacrylate) sample holder (2), specimens of resin-based dental composites (3), rod (4) and PVC tube (5); relationship between loading force and shim thickness of the Rub&Roll machine (C).

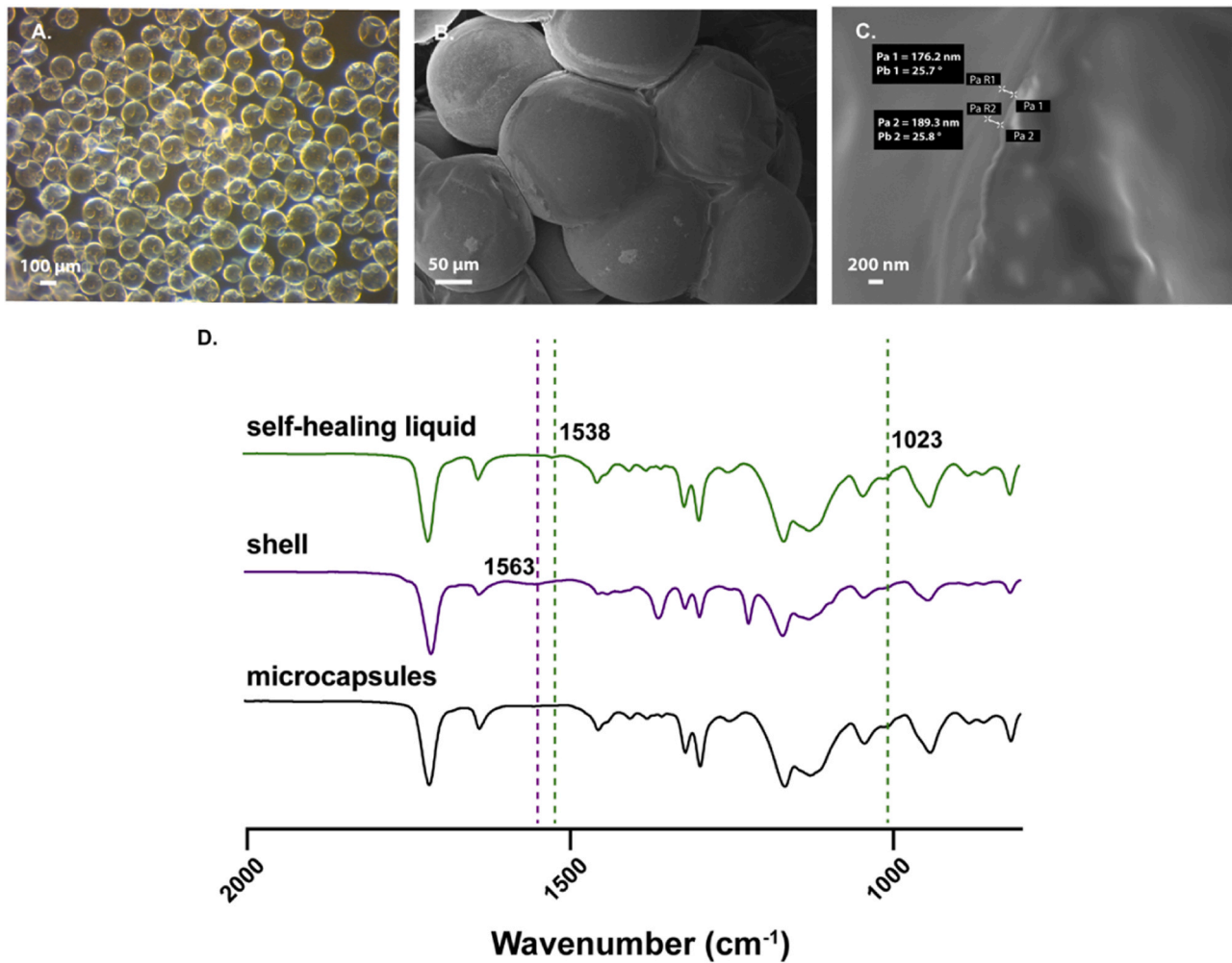


Fig. 2. Light microscopy of microcapsules (A); scanning electron micrograph of the microcapsules (B); electron micrograph of microcapsule shell (C). Fourier-transform infrared spectroscopy (FTIR) of self-healing liquid, shell and microcapsules (D).

$$F = \sum_{j=0}^{j_{\max}} n_j$$

where S_0 is the minimum stress level, j is an integer representing the stress level; at the stress level of j , n_j is the number of specimens in the less happened event. The plus sign (+) in the fatigue strength formula is chosen when survived events happen less than fracture events; the minus sign (-) is chosen for the opposite situation. Scanning electron microscopy was used to check the fracture planes of the fractured samples.

2.6. Fatigue tests in a wear simulation machine (Rub&Roll)

A top view of the interior of Rub&Roll is shown in Fig. 1A. The specimens were fixed to the poly(methyl methacrylate) sample holders (Autoplast cold-curing denture base material, Candulor, Wangen Switzerland) with a dental impression compound material (Kerr, Czech Republic). Next, the length of all sample holders with specimens was fixed at 27.5 mm by a cutting machine (Weiss machine & tools, WMD20LV). A 0.5 mm shim was placed under each sample holder based on the previously recorded relationship between shim thickness and resulting normal forces in the Rub&Roll to adjust the applied maximum loading force to 50 N during fatigue testing in the simulation machine (Fig. 1C). PVC tubes were placed on each loading rod to mimic food chewing. Artificial saliva solution (methyl-p-hydroxybenzoate, sodium

carboxymethylcellulose, KCl, MgCl₂, CaCl₂, K₂HPO₄, KH₂PO₄, pH: 7.2, 600 mL) was added to the simulation machine to provide a wet environment. During the ageing process, the rotation speed of the machine was set at 9 rpm and the contact frequency 0.15 Hz to mimic loading conditions like mastication in clinical situation. The artificial saliva solution and PVC tubes were changed every week. After four weeks of fatigue testing (corresponding to 448,000 loading cycles), the dental impression compound was removed from the specimens, and the flexural strength after the Rub&Roll testing (S_{final}) was measured by using a universal testing machine (MTS, 858 Mini Bionix II) with the three-point-bending test as described above (span: 10 mm) in Section 2.4. Scanning electron microscopy (SEM) was also used to check the fracture plane of the fracture surfaces.

Blocks of around $2.5 \times 2.5 \times 2.5 \text{ mm}^3$ have been scanned using the Multiscale Skyscan 2211 (Bruker, Belgium), at a voxel size of 1.0 μm, 90 kV, 200 μA, 360° rotation, 0.29° rotation step, and 1800 ms exposure time, averaging 3 frames per projection for micro computed tomography. Tomograms were reconstructed using filtered back-projection at NRecon (v. 1.7.4.6, Bruker, Belgium). The separation of air bubbles and initiators/microcapsules was performed using Avizo (FEI Visualization Sciences Group, USA), based on the sphericity of the objects. Calculation of equivalent diameter, percentage of initiators/microcapsules and air bubbles and 3D rendering were also conducted on Avizo.

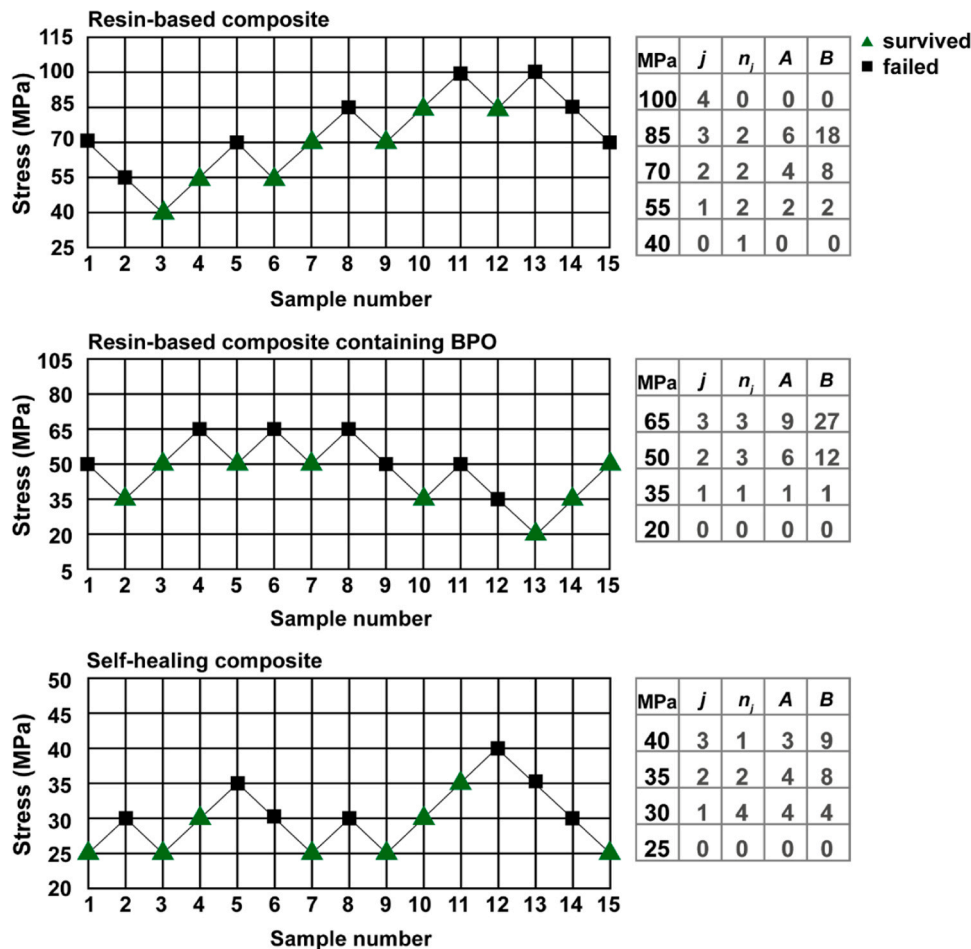


Fig. 3. Staircase fatigue test results for microcapsule-free resin-based composite, microcapsule-free composite containing BPO, and self-healing composite containing microcapsules. (j : the stress level; n_j : the number of specimens in the less happened event at the stress level of j , $A = \sum_{j=0}^{j_{\max}} j \times n_j$, $B = \sum_{j=0}^{j_{\max}} j^2 \times n_j$).

2.7. Statistical analyses

For the groups without ageing and ageing with Rub&Roll, 8 observations were available in each condition. For the staircase method only one value and standard deviation for fatigue strength (FS) were available, for each experimental group. This standard deviation has exactly the same interpretation as the standard error for the groups without ageing or aged with the Rub&Roll. This implies that all comparisons between groups or methods of ageing could be performed with t-tests. These tests were performed both for the absolute decreases in strength as well as for the relative decreases ($(S_{\text{initial}} - S_{\text{final}}) / S_{\text{initial}} \times 100\%$).

3. Results

3.1. Characterization of microcapsules

A representative light microscopy (LM) image of the synthesized microcapsules is shown in Fig. 2A, which reveals that the microcapsules exhibited a regular spherical morphology and had a size of $215 \pm 30 \mu\text{m}$. In addition, representative scanning electron microscopy (SEM) images (Fig. 2B and C) showed a clear microcapsule morphology with a microcapsule shell thickness of around 180 nm.

Characteristic absorption peaks of the self-healing liquid and shell were detected using FTIR in the microcapsules (Fig. 2D). In the FTIR spectrum of the self-healing liquid, the vibration absorption peak at 1538 cm^{-1} was assigned to $=\text{C-H}$ bonds in TEGDMA as well as the vibration of benzene rings in DEPT. The peak at 1023 cm^{-1} was attributed to the bending of the olefin $\text{C}=\text{O}$ vibration from TEGDMA. In the FTIR-

Table 3

Initial flexural strength (S_{initial}), fatigue strength (FS) and results from Student's t-test (p-value and 95% confidence interval (CI)) for comparison between S_{initial} and FS strength for three types of resin-based composites.

| Group name | S_{initial} (MPa, N = 8) | FS (MPa, N = 1) | p | CI |
|---------------------------------------|-----------------------------------|-----------------|--------|---------------|
| Resin-based composite | 139.0 ± 19.5 | 73.2 ± 26.5 | 0.0472 | [1,1...130,5] |
| Resin-based composites containing BPO | 97.7 ± 16.3 | 46.8 ± 12.6 | 0.0079 | [18,1...83,7] |
| Self-healing composites | 50.0 ± 5.5 | 30.4 ± 4.5 | 0.0053 | [8,0...31,3] |

spectrum of the shell, the peak at 1563 cm^{-1} was caused by the amide N-H group. Overall, the FTIR results confirmed that the healing liquid was successfully encapsulated in the PUF microcapsules.

3.2. Staircase fatigue tests

The results of the staircase fatigue tests are shown in Fig. 3. The results of initial flexural strength (S_{initial}) and fatigue strength (FS) are shown in Table 3 and Fig. 4A. As expected, the fatigue strengths (FS) of all groups were significantly lower than the initial strength (S_{initial}) (Table 3, Fig. 4A). The decrease ratio ($(S_{\text{initial}} - \text{FS}) / S_{\text{initial}} \times 100\%$) between fatigue strength relative to the initial strength was shown in Table 4 and Fig. 4B, and there was no significant difference between these three groups. The Scanning electron microscopy (SEM) of the fracture planes of the fractured samples (Fig. 4C, D, and E) indicated that

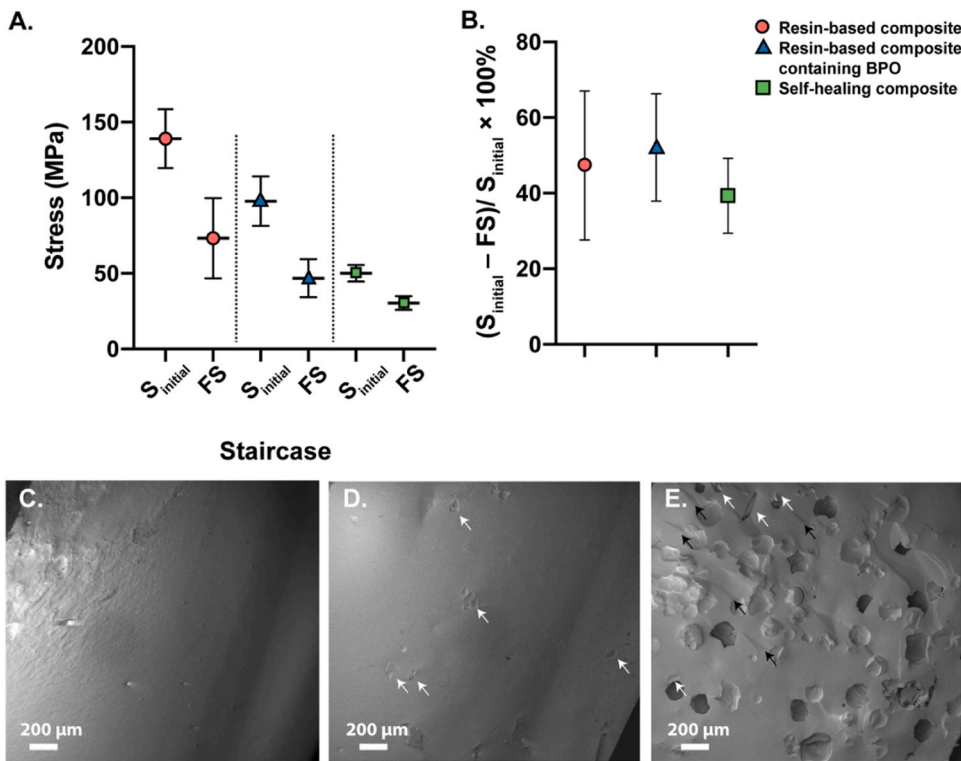


Fig. 4. Comparison between initial flexural strength ($S_{initial}$) and final fatigue strength (FS) after staircase fatigue testing of different resin-based composites (A). The decrease ratio ($(S_{initial} - FS) / S_{initial} \times 100\%$) in three different resin-based composites (B). Scanning electron microscopy of the fracture surface of the fractured specimens: resin-based composite (C); resin-based composite containing BPO (D); self-healing composite containing microcapsules (E). White arrows and black arrows indicate initiator (BPO) particles and stepwise fracture patterns, respectively.

Table 4
Comparisons of the decrease ratio ($(S_{initial} - FS) / S_{initial} \times 100\%$) between three different resin-based composites.

| Group name | $(S_{initial} - FS) / S_{initial} \times 100\%$ (N = 1) | p | CI |
|---|---|--------|------------------|
| Resin-based composite vs. Resin-based composites containing BPO | 47.3 ± 19.7% vs. 52.1 ± 14.2% | 0.8437 | [- 42,8... 52,4] |
| Resin-based composites vs. Self-healing composites | 47.3 ± 19.7% vs. 39.3 ± 9.9% | 0.7150 | [- 35,1... 51,2] |
| Resin-based composites containing BPO vs. Self-healing composites | 52.1 ± 14.2% vs. 39.3 ± 9.9% | 0.4578 | [- 21,0... 46,7] |

Table 5
Initial flexural strength ($S_{initial}$), final flexural strength (S_{final}) and results from Student's t-test (p-value and 95% confidence interval (CI)) for comparison between $S_{initial}$ and S_{final} for three types of resin-based composites.

| Group name | $S_{initial}$ (N = 8) | S_{final} (N = 8) | p | CI |
|---------------------------------------|-----------------------|---------------------|--------|----------------|
| Resin-based composite | 139.0 ± 19.5 MPa | 116.0 ± 23.4 MPa | 0.0509 | [- 0,1...46,1] |
| Resin-based composites containing BPO | 97.7 ± 16.3 MPa | 68.9 ± 23.5 MPa | 0.0129 | [7,1...50,5] |
| Self-healing composites | 50.0 ± 5.47 MPa | 46.5 ± 9.07 MPa | 0.3658 | [- 4,5...11,5] |

the fracture surface of resin-based composite was smooth. In contrast, initiator particles (BPO) were recognizable for resin-based composite containing BPO (indicated by white arrows). For self-healing resin-based composites, initiators (white arrows) and microcapsules could be clearly detected. Stepwise fracture patterns were also clearly visible on the fracture surfaces (black arrows), which indicate the brittle fracture mode of the flowable composites.

3.3. Flexural strength before and after ageing in the Rub&Roll machine

Table 5 and Fig. 5A showed the flexural strength of the composites before ($S_{initial}$) and after (S_{final}) four weeks of ageing in the Rub&Roll simulation machine, respectively. S_{final} decreased to a level of 83% relative to $S_{initial}$ ($p = 0.0509$, CI [-0,1...46,1]) for the resin-based group, close to statistical significance, whereas S_{final} of the resin-based composite containing BPO group significantly decreased to 71% of $S_{initial}$ ($p = 0.0129$, CI [7,1...50,5]). However, S_{final} for the self-healing composite group decreased to a lesser extent (93% relative to $S_{initial}$) compared to the other types of composites upon oral ageing in the Rub&Roll machine ($p = 0.3658$). In addition, the decrease ratios ($(S_{initial} - S_{final}) / S_{initial} \times 100\%$) calculated from the flexural strength of the composites before ($S_{initial}$) and after (S_{final}) four weeks of ageing in the simulation machine were shown in Table 6 and Fig. 5B, and there was no significant difference in the comparisons of the decrease ratio between the three groups. The scanning electron microscopy showed that fracture planes were comparably smooth - characteristic for the brittle fracture of resin-based composites - to the fracture planes as observed upon staircase testing (Fig. 5C, D and E). This outcome evidences that SEM is a qualitative technique that only allows to analyze fracture plans after - but not during - destructive testing.

After four weeks of ageing in the Rub&Roll machine, nano-CT morphological analysis was also applied on the various experimental groups (Fig. 6A, E and I). The initiators/microcapsules and air bubbles were marked as red and green, respectively (Fig. 6B, F and J). Initiator particles and microcapsules were homogeneously distributed throughout the matrix of the resin-based composite containing BPO (Fig. 6G) and self-healing composites (Fig. 6K). The amount of air bubbles was lower in the resin-based composite containing BPO (Fig. 6H) vs. in self-healing composites (Fig. 6L) (0.87% vs. 1.69% of the total volume). The equivalent diameter of the air bubbles in the resin-based composite containing BPO was 53.6 μm [13.7-455.4] μm , whereas in the self-healing composite it was 48.2 μm [5.2-413.7] μm . Microcapsules/initiators (Fig. 6C) and air bubbles (Fig. 6D) were not detected in resin-based composite control specimens. Unfortunately, no

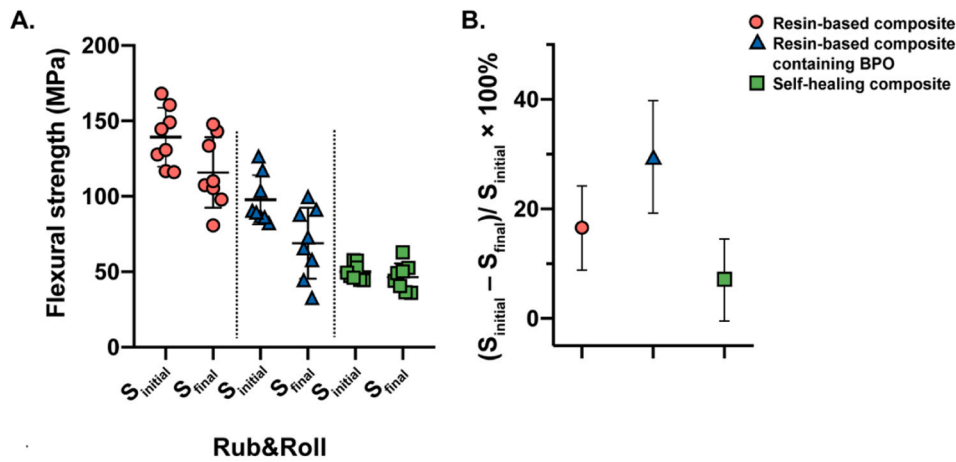


Fig. 5. The flexural strength of resin-based composite, resin-based composite containing BPO, and self-healing composites containing microcapsules before and after ageing in the wear simulating machine (Rub&Roll) (S_{initial} and S_{final} , respectively) (A). The decrease ratio between the final strength to the initial strength ($(S_{\text{initial}} - S_{\text{final}}) / S_{\text{initial}} \times 100\%$) (B). Scanning electron microscopy of the fracture surface of the Rub& Roll-ageing resin-based dental composites after the three-point-bending test: resin-based composite (C); resin-based composite containing BPO (D); self-healing composite containing microcapsules (E). White arrows and black arrows indicate initiator (BPO) particles and stepwise fracture patterns.

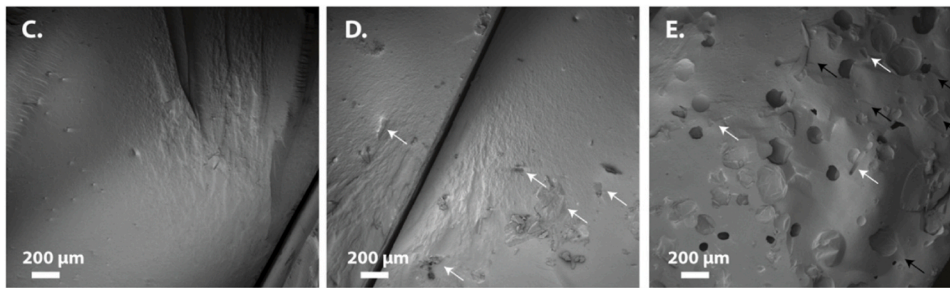


Table 6

Comparisons of the decrease ratio ($(S_{\text{initial}} - S_{\text{final}}) / S_{\text{initial}} \times 100\%$) between flexural strength of the composites before (S_{initial}) and after (S_{final}) for three different resin-based composites.

| Group name | $(S_{\text{initial}} - S_{\text{final}}) / S_{\text{initial}} \times 100\%$ (N = 1) | p | CI |
|---|--|--------|-----------------|
| Resin-based composite vs. Resin-based composites containing BPO | $16.5 \pm 7.7\%$ vs. $29.5 \pm 10.3\%$ | 0.3172 | [-12,4...38,3] |
| Resin-based composites vs. Self-healing composites | $16.5 \pm 7.7\%$ vs. $7.0 \pm 7.5\%$ | 0.3757 | [- 11,6...30,7] |
| Resin-based composites containing BPO vs. Self-healing composites | $29.5 \pm 10.3\%$ vs. $7.0 \pm 7.5\%$ | 0.0785 | [- 2,6...47,5] |

microcracks in the samples could be detected using this technique.

4. Discussion

The objective of this study was to investigate the fatigue resistance of resin-based composite containing microcapsules filled with healing liquid. To this end, we used traditional staircase fatigue tests and a clinically more relevant wear simulation machine (Rub&Roll) to simulate the oral environment through cyclic mastication-mimicking loading in the presence of artificial saliva.

In the staircase fatigue test, fatigue resistance primarily depends on the presence of material flaws [30]. Therefore, the staircase fatigue test based on prolonged cyclic loading of test specimens is a well-established method to create microcracks and evaluate their effect on mechanical performance. Similar to previous studies, self-healing composites containing microcapsules displayed a considerably reduced flexural strength [8,12]. Therefore, it can be concluded that the 10,000 loading cycles under the current experimental conditions were sufficient to reduce the mechanical properties of all resin-based dental composites by inducing the formation and growth of microcracks, as reflected by a

decreased ratio of the final vs. initial flexural strength of between 39% and 52%. No differences were observed between the various groups, indicating that the staircase test did not discriminate between the tested composites regarding their long-term fatigue behaviour. From the SEM photos of the fracture planes, stepwise fracture patterns were clearly visible on the fracture surfaces of the self-healing dental composite, which are indicative of the brittle fracture mode of the flowable composites, even for self-healing composites containing microcapsules.

Although a staircase fatigue test is an efficient way to evaluate the fatigue behaviour of dental composites, it should be stressed that the cyclic loading stresses applied in such tests are much higher than physiological loading in the oral environment [31]. From the strong reductions in relative strength as described above (39–52%), it can be concluded that the staircase method was too severe to reveal potential improvements regarding fatigue resistance of the self-healing composites. This excessive loading might have compromised the self-healing efficiency of the microcapsules by forming microcracks that were too large to be healed by healing liquid flowing from fracture microcapsules.

A wear simulating machine (Rub&Roll) was used in this study to apply a mild cyclic loading under wet conditions to the resin-based composites to mimic the physiological conditions of the oral environment more closely. Flexural strength clearly decreased for resin-based composites and resin-based composites containing BPO after 4 weeks in the Rub&Roll due to a combination of water ageing (4 weeks) and cyclic loading (corresponding to 5 years of clinical mastication cycles). In a previous study on static ageing of resin-based composites in water (2 years), the flexural strength of resin-based dental composites depended on curing time, filler concentration, and concentration of silane coupling agents, but the influence of water ageing on flexural strength was marginal [32]. However, our results indicate that cyclic loading under wet conditions as exerted by the Rub&Roll led to further deterioration of the flexural strength of the resin-based composites. These results seem to indicate that traditional static ageing in water does not reflect the complexity of physiological mastication. In contrast, cyclic loading under wet conditions appears to be a clinically more relevant test method to study the long-term performance of resin-based conditions.

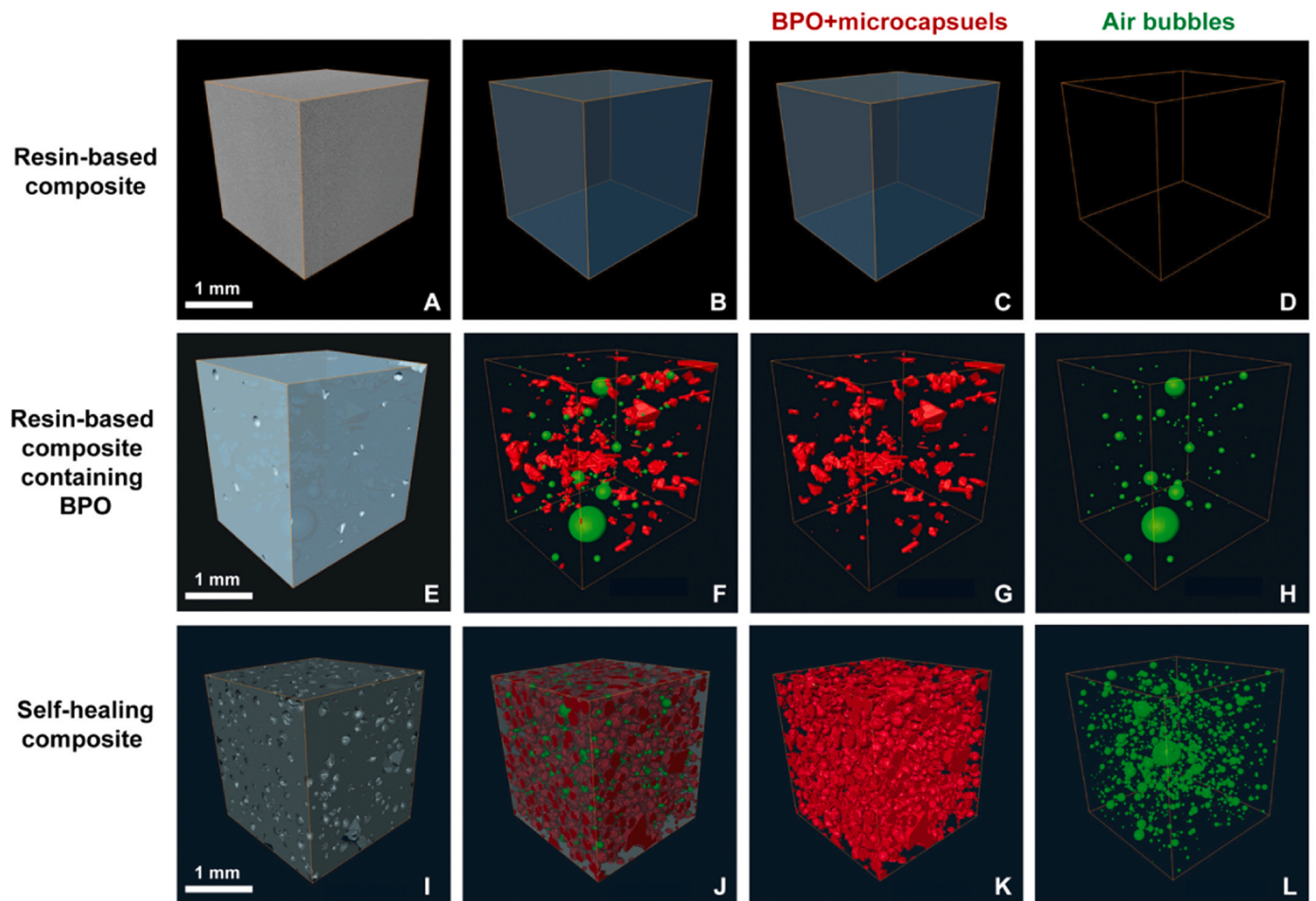


Fig. 6. Nano-CT images of resin-based dental composites after four weeks of ageing in the wear simulating machine (Rub&Roll): resin-based composite (A-D); resin-based composite containing BPO (E-H); self-healing composite containing microcapsules (I-L). BPO and microcapsules were marked with red (C, G and K) and air bubbles were marked with green (D, H and L).

However, the flexural strength of self-healing composites was not reduced upon cyclic loading under wet conditions in the Rub&Roll machine. Therefore, it can be concluded that self-healing composites containing microcapsules improved the fatigue resistance of the resin-based dental composites. This can be explained by several factors. Firstly, in this study, we used microcapsules around $215 \pm 30 \mu\text{m}$, which could rupture efficiently when microcracks approached the microcapsules due to the suitable shell strength and fluid pressure of the microcapsules. In other words, the force creating the microcracks within the Rub&Roll machine matched the force required to break the microcapsules [12]. Secondly, the relatively mild cyclic loading condition created by Rub&Roll machine provided enough healing time for the self-healing system. Evidently, cyclic loading upon staircase testing was more extreme and challenging for the resin-based composites, while the milder testing conditions upon cyclic loading under wet conditions in the Rub&Roll led to efficient healing of microcracks and prevention of the formation of large microcracks. In addition, we showed that self-healing dental composites effectively resisted water ageing when exposed to artificial saliva in the Rub&Roll. These results were in line with previous studies which concluded that the self-healing efficiency and fracture toughness were not affected by static water ageing for up to six months [11]. Self-healing of dental resin-based composites facilitated by the incorporation of microcapsules filled with healing liquids resulted in efficient healing, even under highly wet conditions [11]. It should be noted that we did not apply a silanization treatment to the microcapsules. Our previous SEM analysis confirmed that the microcapsules were well connected to the surrounding resin matrix of the

commercial flowable composite [12]. This qualitative observation was confirmed by the effective self-healing under static and cyclic conditions (current study), which indicates that the bonding between the microcapsule shell and the bisphenol A-glycidyl methacrylate based light-cured composite was sufficiently strong - and the microcapsule shell strength sufficiently low - to allow for rupture of these microcapsules and local release of the healing liquids in forming microcracks [12].

However, the incorporation of microcapsules inevitably led to considerably reduced initial flexural strength values of resin-based composite. This outcome was in agreement with previous studies on self-healing composites containing microcapsules, which showed that enhanced microcapsule and/or initiator contents decreased the flexural strength and/or fracture toughness of these composites [8,9,11,12]. It is logical that resin-based composites' flexure strength or fracture toughness decreased upon incorporating mechanically weak microcapsules containing healing liquids. The nano-CT analysis of the various resin-based composites revealed a second mechanism by which self-healing composites were weakened upon introducing self-healing microcapsules. Undesirably, manual mixing of BPO and microcapsules with flowable composite introduced high amounts of air bubbles of diameters range between different diameters, which undoubtedly deteriorate the mechanical properties of those samples. In view of the negative effects of the inherent weakness of microcapsules and the abundant microporosity introduced upon manual mixing of microcapsules and BPO with the resin matrix, the self-healing dental composites developed herein evidently do not yet meet clinical requirements. Therefore, future

studies on self-healing resin-based composites should aim at improving the mechanical properties of the initial self-healing dental composites without compromising their self-healing efficacy. Based on the current findings in our study, a delicate balance between microcapsule mechanical properties and self-healing efficiency should be identified to minimize these negative effects of microcapsules containing healing liquids as much as possible. Additionally, a more efficient method to incorporate microcapsules without introducing air bubbles could strongly improve the mechanical properties of the resulting self-healing dental composite. Overall, we have confirmed the promise of self-healing dental composites to improve their fatigue performance, but clinical applicability is still challenging due to the above-described reduction in mechanical strength as well as additional challenges that should be overcome, such as the biocompatibility of the healing liquid that might be released into the oral cavity upon excessive polishing, handling, etc. Besides the possible improvements in material, human saliva will be chosen as a wet condition in Rub&Roll machine to better mimic the oral environment wear condition, after the current machine can overcome the contamination problems of the human saliva during long-time ageing.

5. Conclusion

Self-healing composites containing microcapsules filled with acrylic healing liquids exhibit enhanced fatigue resistance under wet conditions in a wear simulation machine (Rub&Roll). Two different types of fatigue tests were applied on our self-healing dental composites, which provided a valuable insight into the self-healing ability of these novel dental composites under dynamic loading conditions. Future research should be focused on the improvement of mechanical properties of self-healing dental composites without compromising their self-healing capacity and biocompatibility to meet the requirement of clinical applications.

References

- [1] Opdam N, Skupien JA, Kreulen CM, Roeters J, Loomans B, Huysmans MD. Case report: a predictable technique to establish occlusal contact in extensive direct composite resin restorations: The DSO-technique. *Oper Dent* 2016;41(S7):S96–108.
- [2] Cho K, Rajan G, Farrar P, Prentice L, Prusty BG. Dental resin composites: A review on materials to product realizations, Composites Part B: Engineering 2022;230: 109495.
- [3] Opdam NJM, van de Sande FH, Bronkhorst E, Cenci MS, Bottenberg P, Pallesen U, et al. Longevity of posterior composite restorations: a systematic review and meta-analysis. *J Dent Res* 2014;93(10):943–9.
- [4] Small ICB, Watson TF, Chadwick AV, Sidhu SK. Water sorption in resin-modified glass-ionomer cements: An in vitro comparison with other materials. *Biomaterials* 1998;19(6):545–50.
- [5] Drummond JL. Degradation, fatigue, and failure of resin dental composite materials. *J Dent Res* 2008;87(8):710–9.
- [6] Kanu NJ, Gupta E, Vates UK, Singh GK. Self-healing composites: A state-of-the-art review. *Compos Part A: Appl Sci Manuf* 2019;121:474–86.
- [7] Van Nieuwenhuysen JP, D'Hoore W, Carvalho J, Qvist V. Long-term evaluation of extensive restorations in permanent teeth. *J Dent* 2003;31(6):395–405.
- [8] Wu J, Weir MD, Melo MA, Xu HH. Development of novel self-healing and antibacterial dental composite containing calcium phosphate nanoparticles. *J Dent* 2015;43(3):317–26.
- [9] Wu J, Weir MD, Zhang Q, Zhou C, Melo MA, Xu HH. Novel self-healing dental resin with microcapsules of polymerizable triethylene glycol dimethacrylate and N,N-dihydroxyethyl-p-toluidine. *Dent Mater* 2016;32(2):294–304.
- [10] Wu T, Gan X, Zhu Z, Yu H. Aging effect of pH on the mechanical and tribological properties of dental composite resins. *Part Sci Technol* 2018;36(3):378–85.
- [11] Wu J, Weir MD, Melo MA, Strassler HE, Xu HH. Effects of water-aging on self-healing dental composite containing microcapsules. *J Dent* 2016;47:86–93.
- [12] Ning K, Loomans B, Yeung C, Li J, Yang F, Leeuwenburgh S. Influence of microcapsule parameters and initiator concentration on the self-healing capacity of resin-based dental composites. *Dent Mater* 2021;37(3):403–12.
- [13] Wu J, Xie X, Zhou H, Tay FR, Weir MD, Melo MAS, et al. Development of a new class of self-healing and therapeutic dental resins. *Polym Degrad Stab* 2019;163: 87–99.
- [14] Jabbari YSA, Mparmpagadaki A, Zinelis S, Eliades G. Assessment of fatigue parameters of dental resin composites using dynamic fatigue testing. *J Compos Mater* 2012;47(4):419–24.
- [15] Bijelic-Donova J, Garoushi S, Vallittu PK, Lassila LV. Mechanical properties, fracture resistance, and fatigue limits of short fiber reinforced dental composite resin. *J Prosthet Dent* 2016;115(1):95–102.
- [16] Arola D. Fatigue testing of biomaterials and their interfaces. *Dent Mater* 2017;33(4):367–81.
- [17] Yahyazadehfard M, Huyang G, Wang X, Fan Y, Arola D, Sun J. Durability of self-healing dental composites: A comparison of performance under monotonic and cyclic loading. *Mater Sci Eng C Mater Biol Appl* 2018;93:1020–6.
- [18] Lohbauer U, v.d. Horst T, Frankenberger R, Krämer N, Petschelt A. Flexural fatigue behavior of resin composite dental restoratives. *Dent Mater* 2003;19(5):435–40.
- [19] Ekaputra IMW, Dewa RT, Haryadi GD, Kim SJ. Fatigue strength analysis of S34MnV steel by accelerated staircase test. *Open Eng* 2020;10(1):394–400.
- [20] Sideridou ID, Karabela MM, Vouvoudi EC. Physical properties of current dental nanohybrid and nanofill light-cured resin composites. *Dent Mater* 2011;27(6): 598–607.
- [21] Aghazadeh Mohandesi J, Rafiee MA, Barzegaran V, Shafiei F. Compressive fatigue behavior of dental restorative composites. *Dent Mater J* 2007;26(6):827–37.
- [22] Soderholm K-JM, Roberts MJ. Influence of water exposure on the tensile strength of composites. *J Dent Res* 1990;69(12):1812–6.
- [23] Ruben JL, Roeters FJM, Montagner AF, Huysmans MCDNJM. A multifunctional device to simulate oral ageing: the "Rub&Roll". *J Mech Behav Biomed Mater* 2014; 30:75–82.
- [24] Lima VP, Crins LAMJ, Bronkhorst EM, Opdam NJM, Ruben JL, Huysmans MCDNJM, et al. P6 - Deterioration of composite restorations in tooth wear patients: translational approach. *Dent Mater* 2022;38:e56–7.
- [25] Ruben JL, Roeters FJM, Truin GJ, Loomans BAC, Huysmans MCDNJM. Cup-shaped tooth wear defects: more than erosive challenges? *Caries Res* 2019;53(4):467–74.
- [26] Ruben JL, Truin GJ, Loomans BAC, Huysmans M. Mimicking and measuring occlusal erosive tooth wear with the "Rub&Roll" and non-contact profilometry. *J Vis Exp* 2018;132.
- [27] Zhang H, Wang X. Fabrication and performances of microencapsulated phase change materials based on n-octadecane core and resorcinol-modified melamine-formaldehyde shell. *Colloids Surf A Physicochem Eng Asp* 2009;332(2–3):129–38.
- [28] Tekce N, Demirci M, Tuncer S, Guder G, Sancak EI. Clinical performance of direct composite restorations in patients with amelogenesis imperfecta - anterior restorations. *J Adhes Dent* 2022;24(1):77–86.
- [29] Monteiro JB, Riquieri H, Prochnow C, Guillard LF, Pereira GKR, Borges ALS, et al. Fatigue failure load of two resin-bonded zirconia-reinforced lithium silicate glass-ceramics: Effect of ceramic thickness. *Dent Mater* 2018;34(6):891–900.
- [30] Dixon WJ, Mood AM. A method for obtaining and analyzing sensitivity data. *J Am Stat Assoc* 1948;43(241):109–26.
- [31] Draughn RA. Compressive fatigue limits of composite restorative materials. *J Dent Res* 1979;58:1093–6.
- [32] Ferracane JL, Berge HX, Condon JR. In vitro aging of dental composites in water—Effect of degree of conversion, filler volume, and filler/matrix coupling. *J Biomed Mater Res* 1998;42(3):465–72.